THE JOURNAL OF BIOLOGICAL CHEMISTRY VOL. 291, NO. 14, pp. 7774–7785, April 1, 2016

Organophosphate Hydrolase Is a Lipoprotein and Interacts with P_i-specific Transport System to Facilitate Growth of *Brevundimonas diminuta* Using OP Insecticide as Source of Phosphate*

Received for publication, January 11, 2016, and in revised form, February 7, 2016 Published, JBC Papers in Press, February 9, 2016, DOI 10.1074/jbc.M116.715110

Sunil Parthasarathy[‡1], Hari Parapatla[‡], Aparna Nandavaram[‡], Tracy Palmer[§], and Dayananda Siddavattam[‡2]

From the [‡]Department of Animal Biology, School of Life Sciences, University of Hyderabad, Hyderabad, 500 046, India and the [§]Division of Molecular Microbiology, College of Life Sciences, University of Dundee, Dundee, United Kingdom

Organophosphate hydrolase (OPH), encoded by the organophosphate degradation (*opd*) island, hydrolyzes the triester bond found in a variety of organophosphate insecticides and nerve agents. OPH is targeted to the inner membrane of *Brevundimonas diminuta* in a pre-folded conformation by the twin arginine transport (Tat) pathway. The OPH signal peptide contains an invariant cysteine residue at the junction of the signal peptidase (Spase) cleavage site along with a well conserved lipobox motif. Treatment of cells producing native OPH with the signal peptidase II inhibitor globomycin resulted in accumulation of most of the pre-OPH in the cytoplasm with negligible processed OPH detected in the membrane. Substitution of the conserved lipobox cysteine to serine resulted in release of OPH into the periplasm, confirming that OPH is a lipoprotein. Analysis of purified OPH revealed that it was modified with the fatty acids palmitate and stearate. Membrane-bound OPH was shown to interact with the outer membrane efflux protein TolC and with PstS, the periplasmic component of the ABC transporter complex (PstSACB) involved in phosphate transport. Interaction of OPH with PstS appears to facilitate transport of P_i generated from organophosphates due to the combined action of OPH and periplasmically located phosphatases. Consistent with this model, *opd* null mutants of *B. diminuta* failed to grow using the organophosphate insecticide methyl parathion as sole source of phosphate.

Membrane-associated organophosphate hydrolase (OPH)[3] hydrolyzes the triester bond found in a variety of organophosphate insecticides and nerve agents (1, 2). The 39-kDa monomer requires Zn^{+} ions as cofactor (3). OPH is encoded by the *opd* (organophosphate degrading) gene found on dissimilar plasmids and the *opd* gene has recently been shown to be a part of an integrative mobilizable element (IME) (4). Due to the mobile nature of the *opd* island, identical *opd* genes are found among bacterial strains isolated from different geographical regions (4, 5). Although its physiological substrate is unknown, OPH hydrolyzes paraoxon at a rate approaching the diffusion limit (k_{cat}/K_m 10^8 M^{-1} s^{-1}) (6). Considering its catalytic efficiency and broad substrate range, it has been assumed that OPH has evolved to degrade organophosphate (OP) insecticides accumulated in agricultural soils (7). Structural analysis shows that OPH contains a TIM barrel-fold as seen in most of the members of amidohydrolase superfamily proteins (8).

OPH associates with cell membranes and membrane-associated OPH has been purified from a number of sources (3, 9–13). Analysis of the amino acid sequences of OPH proteins indicates that all of them contain a predicted signal peptide harboring a well defined twin-arginine (Tat) motif. Twin-arginine signal peptides serve to target proteins to the twin-arginine protein transport (Tat) pathway, which translocates folded proteins across the bacterial cytoplasmic membrane (14). Proteinase K treatment confirmed that OPH is exported to the periplasmic side of the inner membrane in *Brevundimonas diminuta* and dependence on the Tat pathway was demonstrated because substitution of the invariant arginine residues of the Tat signal peptide affected both processing and localization of OPH (15). However, the mechanism by which OPH is anchored to the inner membrane and the physiological role of OPH are currently unclear. In this report we demonstrate that OPH is a lipoprotein and that it plays an essential role in the acquisition of phosphate from OP insecticides.

Experimental Procedures

Media, Strains, and Plasmids—Strains and plasmids used in the present work are shown in Table 1. Primers used for PCR amplification and site-directed mutagenesis are listed in Table 2. *B. diminuta* cultures were grown either in LB medium or in HEPES minimal medium. HEPES minimal medium was pre-

* This work was supported in part by the Department of Biotechnology, Govt. of India (to D. S. Laboratory). Department of Animal Biology was supported by the DST-FIST (Department of Science and Technology–Fund for Improvement of S&T Infrastructure), and the School of Life Sciences, University of Hyderabad is supported by DBT-CREBB/BUILDER (Department of Biotechnology–Centre for Research and Education in Biology and Biotechnology/Boost to University Interdisciplinary Life Science Departments for Education and Research). The authors declare that they have no conflicts of interest with the contents of this article.

[1] Supported by a Shantha Biotechnics Junior Research Fellowship (JRF) and Commonwealth Split-Site Fellowships, British Council, UK.

[2] To whom correspondence should be addressed: Dept. of Animal Biology, School of Life Sciences, University of Hyderabad, Prof. C. R. Rao Rd., Gachibowli, Hyderabad 500 046, India. Tel.: 91-40-23134578; Fax: 91-40-23010120/145; E-mail: sdsl@uohyd.ernet.in.

[3] The abbreviations used are: OPH, organophosphate hydrolase; OP, organophosphate insecticides; Tat, Twin arginine transport; SPase, signal peptidase;DDM,*n*-dodecyl β-D-maltoside;Tricine,*N*-[2-hydroxy-1,1-bis(hydroxymethyl)ethyl]glycine; IMAC, immobilized-metal affinity chromatography; BN-PAGE, blue native-PAGE.

TABLE 1
Strains and plasmids used in the study

	Description	Reference
Strains		
E. coli DH5α	*λsupE44 ΔlacU169 (Δ80 lacZΔM15) hsdR17 recA1 endA1 gyrA96 thi1 relA1*	50
E. coli BL21	*hsdS gal (ΔcIts857 ind1 Sam7 nin5) lacUV5 T7 gene1*	51
E. coli S17–1	*thi pro hsd Rhsd MrecA RP4 2-Tc::Mu-Km^r::Tn7 (Tp^r, Sp^r, Sm^r)*	52
BTH101	*F cya-99 araD139 galE15 galK16 rpsL1 (Strr) hsdR2 mcrA1 mcrB1*	53
ArcticExpress	*E. coli B F$^-$ ompT hsdS (r_B^- m_B^-) dcm$^+$ Tet^r gal endA Hte (cpn10 cpn60 Gent^r)*	Agilent Technologies
B. diminuta	Sm^r, PmB^r, *opd*$^+$	11
B. diminuta DS010	Sm^r, Tc^r, PmB^r, *opd*$^-$ (*opd*::*tet*)	15
Plasmids		
pMMB206	Cm^r, broad host range, low copy number, expression vector	54
pGEMT-Easy	Amp^r, TA cloning vector	Promega
pTZ57 R/T	Amp^r, TA cloning vector	Fermentas
pET23b	Amp^r, T7 promoter and a C-terminal His_6 tag	Novagen
pETduet1	Amp^r, contains two multiple cloning sites downstream of T7 promoter.	Novagen
pRSETA	Amp^r, T7 promoter and a N-terminal His_6 tag	Thermo Scientific
pSM5	Cm^r, complete *opd* gene encoding preOPH, cloned in pMMB206 as EcoRI and HindIII fragment	13, 46
pKNT25	Plasmid for the expression of C-terminal T25-fusion proteins (Kan^r)	31
pUT18C	pUT18C Plasmid for the expression of N-terminal T18-fusion proteins (Amp^r)	31
pCSOPH	Cm^r, derivative of pSM5 encoding OPH^{C24S}	This work
pOPH141HIS	Cm^r, derivative of pSM5 encoding OPH with 10 histidine residues between 141–142 residues.	This work
pUT18COPH	Amp^r, complete *opd* gene cloned inframe to code for C-terminal T18 fragment.	This work
pUT18CPstS	Amp^r, complete *pstS* gene cloned inframe to code for C-terminal T18 fragment.	This work
pKNT25OPH	K_m^r, complete *opd* gene cloned inframe to code for N-terminal T25 fragment.	This work
pKNT25PstS	K_m^r, complete *pstS* gene cloned inframe to code for N-terminal T25 fragment.	This work
pOPHV400	Cm^r, Avi tag coding sequence inserted as XhoI and HindIII fragment in pSM5, codes for OPH^{CAviTag}	This work
pAVB400	Amp^r, *opd* variant coding OPH^{CAviTag} taken as EcoRI and HindIII fragment from pOPHV400 and cloned into one of the two multiple cloning sites of pETduet1. The *birA* gene amplified from *E. coli* as NdeI and XhoI fragment was cloned in the second multiple cloning site. Codes for OPH^{CAviTag}, and BirA ligase.	This work
pPST300	Amp^r, the *pstS* amplified from *B. diminuta* as NdeI and XhoI fragment was cloned in pET23b. Codes for PstS^{N6His}	This work
pLPST300	Cm^r, *pstS* amplified from pPST300 as BglII and HindIII fragment cloned in pMMB206 digested with BamHI and HindIII.	This work
pTOLC400	Amp^r, The *tolC* gene amplified from *B. diminuta* cloned as BglII and EcoRI fragment in pRSETA. Codes for TolC^{N6His}	This work
pTLOPH	Cm^r, the *opd* gene amplified as EcoRI and HindIII fragment cloned in pMMB206. Codes for untagged OPH under control of the *tac* promoter.	This work

TABLE 2
Primers used in the study
The bold case indicates respective restriction sites.

Primer name	Sequence	Appending sites
C24S FP	GGCCTGGCTGGGTCCCGCGAGCGTGGCTG	Forward primer used to introduce serine in place of cysteine at 24th position
C24S RP	CAGCCACGCTCGCGGGATCCCAGCCAGGCC	Reverse primer used to introduce serine in place of cysteine at 24th position
140bamHI FP	TCGATGCGATTG**GGATCC**GTAGAGGAACTCA	Forward primer used to create *BamH*I site at 426th nucleotide position
140bamHI RP	TGAGTTCCTCTAC**GGATCC**CAATCGCATCGA	Reverse primer used to create *BamH*I site at 426th nucleotide position
10x HIS FP bglII	GCGC**AGATCT**CACCACCACCACCACCACCACCACCACCACCACAGATCTGCGC	Forward primer coding for 10 histidine residues with BglII site
10x HIS RP bglII	GCGC**AGATCT**GTGGTGGTGGTGGTGGTGGTGGTGGTGAGATCTGCGC	Reverse primer coding for 10 histidine residues with BglII site
PDSIII	GGGTGCGCGGAGCGTG**CATATG**TCGATCGGCACAGGC	Forward primer used to amplify *opd* gene with NdeI site
PDSIV	GGATCCAGATGCTCGAGTGACGCCCGCAAGG	Reverse primer used to amplify *opd* gene with XhoI site
POPD-F	GG**GAATTC**TGCGCGGAGCGTGCATATGTCGATCGGCACAGGC	Forward primer used to amplify *opd* gene with EcoRI site
POPD-R	AACCG**AAGCTT**CAGATGGCGTGAGGGCGG	Reverse primer used to amplify *opd* gene with HindIII site
PstS-F	TGC**CTGCAG**AATGTTCAAGACATTCGCTCCCAAG	Forward primer used to amplify *pstS* with a PstI site
PstS-R	CT**GAATTC**TTTCAGCTCGCTGCCATCCAG	Reverse primer used to amplify *pstS* with a EcoRI site
PstSPET-F	GCGC**CATATG**GCCAAGACATTTGCCCTT	Forward primer used to amplify *pstS* with a NdeI site
PstSPET-R	GCGA**CTCGAG**TTTCAGCACCGACCCGTC	Reverse primer used to amplify *pstS* with a XhoI site
PstSPMB-F	CCC**AGATCT**AGAAATAATTTTT	Forward primer used to amplify *pstS* from pPST300 with a BglII site
PstSPMB-R	CCTT**AAGCTT**CTAGTTATTGCTCAGCGGTGGC	Reverse primer used to amplify *pstS* from pPST300 with a HindIII site
AviTag-F	GCTATC**CTCGAG**GGCCTGAACCGCATCTTCGAGGCTCAGAAAATCGAA	Forward primer coding AviTag with a XhoI site
AviTag-R	GCAGCT**AAGCTT**GCGGCCGCTTAGTGCCATTCGATTTTCTGAGCCTCG	Reverse primer coding AviTag with a HindIII site
BirA-F	GCACA**CATATG**AAGGATAACACCGTGCCACTG	Forward primer used to amplify *birA* from *E. coli* with a NdeI site
BirA-R	CTCCCCT**CTCGAG**TTTTTCTGCAC	Reverse primer used to amplify *birA* from *E. coli* with a XhoI site.
TolCPRT-F	AAA**AGATCT**ACATGAAACCCGTTCGCCG	Forward primer used to amplify *tolC* from *B. diminuta* with a BglII site
TolCPRT-R	AAA**GAATTC**CTATTGGTGCGGCAGGTTGCT	Reverse primer used to amplify *tolC* from *B. diminuta* with a EcoRI site

pared by dissolving 0.2 g of KCl, 0.2 g of $MgSO_4 \cdot 7H_20$, 40 mg of $CaNO_3 \cdot 4H_2O$, 80 mg of $(NH_4)_2HPO_4$, and 1 mg of Fe_2SO_4 in 1 liter of 50 mM HEPES, pH 7.4. The medium also contained an essential amino acid mixture (0.07 mM), pantothenate (0.5 mg), vitamin B-12 (0.001 mg), and biotin (0.001 mg) along with sodium acetate (2%) as carbon source. The $(NH_4)_2HPO_4$ was omitted when methyl parathion (0.6 mM) was used as sole phosphate source. When required, polymyxin (10 μg/ml), chloroamphenicol (30 μg/ml), or tetracycline (20 μg/ml) were supplemented to the growth medium. All chemicals used in this study were procured from Sigma, unless otherwise specified all restriction and other enzymes used in DNA manipulations were from ThermoScientific. Routine DNA manipulations were performed following standard procedures (16).

Carbonate and Urea Extraction—Total membrane preparations were made from *B. diminuta* following standard procedures (17). The cytoplasmic membrane was isolated by following the discontinuous sucrose gradient method described

elsewhere (18) and equal amounts of membrane was resuspended in buffer containing different concentrations of sodium carbonate, pH 11.5, or urea (2–8 M as indicated). After a 1-h incubation at room temperature the samples were centrifuged at 227,226 × *g* using a TLA 120.2 rotor (Beckman coulter) for 45 min to pellet the washed membranes. Detection of OPH in the wash supernatant and membrane fractions was achieved by Western blots using anti-OPH antibodies (15). The quantity of OPH in membrane and supernatant fractions were densitometrically determined by comparing with the OPH signal obtained with untreated membrane.

Globomycin Treatment—The *opd* null mutant, *B. dimimuta* DS010 containing the plasmid pSM5 was grown in LB medium to mid-log phase (0.6 OD at 600 nm) and 50 μg/ml of globomycin (Sigma) was added to the culture medium 1 h before the expression of OPH was induced by addition of 3 mM isopropyl β-D-galactopyranoside (IPTG) (19, 20). After 6 h of induction, the culture was harvested, washed in SET buffer (500 mM sucrose, 5 mM EDTA, and 20 mM Tris-HCl, pH 8.0), and used to prepare periplasmic, cytosolic, and total membrane fractions as described previously (21, 22). OPH-specific signals in the subcellular fractions were detected by performing Western blot analysis.

Generation of OPH^{C24S}—The invariant cysteine residue in the lipobox motif of the OPH signal peptide was modified to serine by performing QuikChange™ site-directed mutagenesis (Stratagene). Plasmid pSM5 was used as template and the cysteine to serine codon substitution was confirmed by sequencing. The resulting plasmid coding for OPH^{C24S} was designated pCSOPH. The *B. diminuta* DS010 (pCSOPH) cultures were grown to mid-log phase and the expression of OPH^{C24S} was induced overnight by supplementation with 3 mM IPTG. The cells expressing OPH^{C24S} were subsequently harvested, washed, and fractionated into periplasm, cytoplasm, and total membrane for the detection of OPH. A similar fractionation procedure was undertaken with *B. diminuta* DS010 (pSM5) to assess membrane anchorage of OPH in wild type cells.

Solubilization of OPH from the Inner Membrane—Inner membrane preparations were isolated from a 10-liter overnight culture of *B. diminuta* following procedures described elsewhere (18). The isolated inner membrane was resuspended in minimal amounts of buffer (20 mM Tris-HCl, pH 8.0, 150 mM NaCl, 2% glycerol) and after estimating the protein concentration the buffer volume was adjusted to give a final protein concentration of 5 mg/ml. Triton X-100 (2 g/g of protein), Triton X-114 (2 g/g of protein), *n*-dodecyl β-D-maltoside (DDM) (1 g/g of protein), and digitonin (8 g/g of protein) were separately added to aliquots of the membrane suspension and samples were incubated with gentle rotation (10 rpm) for 1 h at 4 °C. Subsequently, the samples were subjected to ultracentrifugation (117,000 × *g*) and the clarified supernatants, containing solubilized protein, were removed into prechilled tubes. The detergent-insoluble fraction was resuspended in an equal volume of buffer and the OPH activity was estimated in both detergent-soluble and detergent-insoluble fractions (3). The percent of OPH released from the membrane was calculated by comparing the total OPH activity associated with the untreated membrane. Subsequently, for identification of fatty acids attached to OPH, the protein was solubilized using 1.5% Triton X-100 as it disrupts interactions of OPH with other proteins and facilitates purification of OPH without interacting partners.

Affinity Purification of OPH and Identification of Fatty Acids—For purification of OPH-specific antibodies, 10 mg of pure OPH, purified as described elsewhere (23), was coupled to 400 μl of CNBr-activated Sepharose™ 4B (GE Healthcare) following the manufacturer's protocol. Aliquots of OPH antisera (15) were passed through the OPH-coupled Sepharose column at a flow rate of 0.5 ml per min. The flow-through was collected carefully and reloaded onto the column to ensure complete binding of OPH-specific antibodies to the column. The unbound antibodies and serum proteins were removed by washing the column with 3 column volumes of wash buffer (20 mM Tris-HCl, pH 7.6). The bound anti-OPH antibodies were eluted (0.1 M glycine-HCl, pH 2.5) as 1-ml fractions into prechilled tubes containing 100 μl of 1 M Tris-HCl, pH 9.0, to ensure quick neutralization of the eluate. The antibody fractions were then pooled and dialyzed against coupling buffer (10 mM sodium phosphate, pH 7.2, 150 mM NaCl).

For coupling to protein A/G beads, approximately 1 mg of purified anti-OPH antibodies were mixed with 500 μl of protein A/G-agarose plus beads (ThermoScientific) equilibrated with coupling buffer and kept for 1 h at 4 °C with gentle shaking. The contents were loaded onto a column and the excess unbound antibodies were removed by washing the column with 3 column volumes of coupling buffer. The anti-OPH antibodies bound to protein A/G-agarose beads were covalently linked by adding one column void volume of cross-linking buffer (10 mM sodium phosphate, pH 7.2, 150 mM NaCl), 2.5 mM disuccinimidyl suberate to the column. The column was left for 1 h at room temperature to complete cross-reaction and excess disuccinimidyl suberate was quenched by washing the column with 25 mM Tris-HCl, pH 7.6. The OPH-antibody cross-linked protein A/G-agarose beads were then taken into a clean tube and suspended in 1 ml of prechilled binding buffer (20 mM Tris-HCl, pH 7.6, 150 mM NaCl, 2% glycerol). Immediately, Triton X-100-solubilized membrane proteins of *B. diminuta* were added to the beads and left overnight at 4 °C with head to head rotation. After incubation the contents were loaded onto a column, washed thoroughly with wash buffer, and the bound proteins were then eluted with glycine-HCl, pH 2.5, prior to neutralization with 100 mM Tris-HCl, pH 9.0. About 100 μg of immunopurified OPH was esterified using methanolic-HCl (24). The fatty acid methyl esters generated from OPH were then analyzed using Agilent GC/MS equipped with a quadrupole mass selective detector. Control samples were prepared from the periplasmic fraction of *B. diminuta* DS010 (pCSOPH) and treated identically to identify the fatty acid methyl esters.

Identification of the OPH Interactome—To identify interacting proteins, OPH was affinity purified using two different approaches. Before proceeding with the purification of OPH, the cell pellet collected from wild type *B. diminuta* was resuspended in PBS buffer (1 g/10 ml) before treatment with 25 mM formaldehyde (25, 26). The formaldehyde cross-linked cell pellet was sonicated (10 cycles of 20-s ON and 40-s OFF) and the

membrane fraction was isolated following established procedures (27). The membrane pellet was extracted three times with 5 ml of chloroform:methanol (1:3) and the precipitated proteins were resolubilized in phosphate buffer (0.1 M phosphate buffer, pH 7.6, 350 mM NaCl, 5% glycerol, 1% DDM, and 50 mM imidazole). The first approach involved immunopurification using anti-OPH antibody cross-linked protein A/G-agarose beads. The resolubilized cross-linked OPH complex was passed through the column containing the antibody-linked beads at a flow rate of 0.5 ml/min. The flow-through was repeatedly passed through the column until negligible amounts of OPH was detected in the flow-through sample. After washing the column with 3 column volumes of wash buffer (20 mM Tris-HCl, pH 7.6, 150 mM NaCl, 2% glycerol, 0.1% DDM), the bound cross-linked OPH complex was eluted as described above, and subsequently analyzed both under native and denaturing conditions. Blue native-PAGE (28) and gel filtration (Superose 6, 10/300 GL, GE Healthcare) were performed to assess the molecular mass of the OPH complex. Tricine-PAGE (29) was performed to visualize polypeptides coeluting with OPH.

In an alternative approach, a deca-histidine-tagged OPH variant (OPH^{10xHis}) was generated. To achieve this, a DNA fragment encoding 10 histidine residues was introduced into the *opd* gene, between nucleotide positions 420 and 426 that encodes amino acids in a loop region of OPH. First, a BamHI restriction site was introduced into *opd* by performing QuikChange mutagenesis between nucleotide positions 420 and 426 using plasmid pSM5 as template. Next, the synthetic DNA fragment encoding the 10 histidine residues was prepared as a BglII fragment and inserted in-frame into the *opd* gene at the generated BamHI site. The resultant plasmid was designated pOPH141HIS. Plasmid pOPH141HIS was mobilized into *B. diminuta* DS010, and *B. diminuta* DS010 (pOPH141HIS) cells were then induced to express OPH^{10xHis} by addition of IPTG at a final concentration of 3 mM. After incubation with IPTG for 5 h the cells were harvested and the cell pellet was resuspended in PBS buffer (1 g/10 ml) and treated with 25 mM formaldehyde to cross-link OPH. The formaldehyde cross-linked cell pellet was processed as described earlier to obtain total membrane pellet. The pellet was then extracted three times with 5 ml of chloroform:methanol (1:3) and the precipitated proteins were resolubilized before loading the soluble proteins onto a nickel-charged immobilized metal affinity chromatography (IMAC). Following washing with phosphate buffer, bound protein was eluted with 500 mM imidazole in phosphate buffer and analyzed both on blue native and Tricine-PAGE. The affinity purified OPH complexes were subjected to tryptic digestion and mass spectrometry (LTQ-Orbitrap XL ETD mass spectrometer) as described elsewhere (30) to establish the identity of OPH interacting proteins.

Bacterial Two-hybrid System—Protein-protein interactions were studied by the bacterial two-hybrid system (BACTH, Euromedex) following protocols described elsewhere (31). The T25 and T18 domains were separately fused to the N or C termini of the target proteins (OPH and PstS). The fusions were produced independently by cloning the *opd* and *pstS* genes in either pKNT25 or pUT18C. Cells of *Escherichia coli* strain BTH101 (Euromedex) were transformed with different combinations of fusion plasmids *i.e.* pUT18CPstS-pKNT25OPH and pUT18COPH-pKNT25PstS. The combinations pUT18CPstS-pKNT25 and pUT18COPH-pKNT25 served as controls. β-Galactosidase assay was performed as described elsewhere (32).

Pulldown Assay of Coexpressed Proteins—Interaction of OPH with a phosphate-binding protein, PstS, and a efflux pump component, TolC, was determined by performing coexpression pulldown assays (33). Initially, an *opd* gene variant engineered to code for OPH with C-terminal AviTag was generated. Two complementary oligos specifying the AviTag sequence (AviTag-F and AviTag-R; Table 2) were annealed, digested with XhoI and HindIII, and cloned into similarly digested plasmid pSM5 to give plasmid pOPHV400, this procedure results in insertion of the AviTag coding sequence in-frame with *opd*. Next, the *opd* gene from plasmid pOPHV400 was excised as an EcoRI and HindIII fragment and cloned into one of the multiple cloning sites of pETduet1 vector that had been similarly digested. Subsequently, the *birA* gene was cloned as an NdeI and XhoI fragment into the second multiple cloning site of this construct. The cloning strategy places *birA* under control of the T7 promoter, allowing for regulatable expression of biotin ligase, the enzyme required to ligate biotin at the conserved lysine residue of the AviTag. The resulting pETduet1 derivative, designated pAVB400, codes for both $OPH^{CAviTag}$ and the biotin ligase. The *pstS* gene was amplified from *B. diminuta* and cloned initially in pET23b as an NdeI-XhoI fragment. The generated recombinant plasmid, pPST300, codes $PstS^{C6His}$. After confirming expression of $PstS^{C6His}$, *pstS* was amplified from pPST300 using primers PstSPMB-F and PstSPMB-R, respectively, and cloned into similarly digested pMMB206 to give plasmid pLPST300, which encodes $PstS^{C6His}$ controlled by the *tac* promoter of the vector. *E. coli* ArcticExpress cells harboring pAVB400 were transformed with pLPST300 and the expression of $OPH^{CAviTag}$ and $PstS^{C6His}$ was induced following standard procedures. The total cell lysate was prepared and the clear lysate was used to isolate $OPH^{CAviTag}$ and any interacting partners using streptavidin magnetic beads (Dynabeads M-280 Streptavidin, Invitrogen) following the manufacturer's protocols. The proteins bound to magnetic beads were analyzed by 12.5% SDS-PAGE and probed either with anti-OPH or anti-His antibodies to detect $OPH^{CaviTag}$ and $PstS^{C6His}$. Cell lysates prepared either from ArcticExpress (pAVB400) or ArcticExpress (pLPST300) cells treated in a similar manner served as controls.

OPH-TolC Interactions—The *tolC* gene was amplified from *B. diminuta* and cloned as a BglII-EcoRI fragment into similarly digested pRSETA. As the cloning strategy facilitates in-frame fusion of the vector-specified His tag to *tolC*, the resulting recombinant plasmid, pTOLC400, codes for $TolC^{N6His}$. Similarly, the *opd* gene was amplified from *B. diminuta* as an EcoRI-HindIII fragment and cloned into similarly digested pMMB206. The resulting recombinant plasmid, pTLOPH, codes for OPH without any affinity tag, expressed under control of the *tac* promoter. The $TolC^{N6His}$ and OPH were coexpressed by adding 1 mM IPTG to the mid-log phase cultures of ArcticExpress (pTLOPH400 + pTOLC400). Similarly, the expression of $TolC^{N6His}$ and OPH were induced from ArcticExpress (pTLOPH400) and ArcticExpress (pTLOPH400) cells before

preparing clear lysate (4 ml) from 50 ml of culture. The lysate was then incubated overnight with 20 μl of MagneHis beads (Promega) at 4 °C with constant mixing. After incubation, the beads were collected and washed following the manufacturer's protocol and the presence of $TolC^{N6His}$ and OPH were detected by performing immunoblots probed either with anti-OPH or anti-His antibodies.

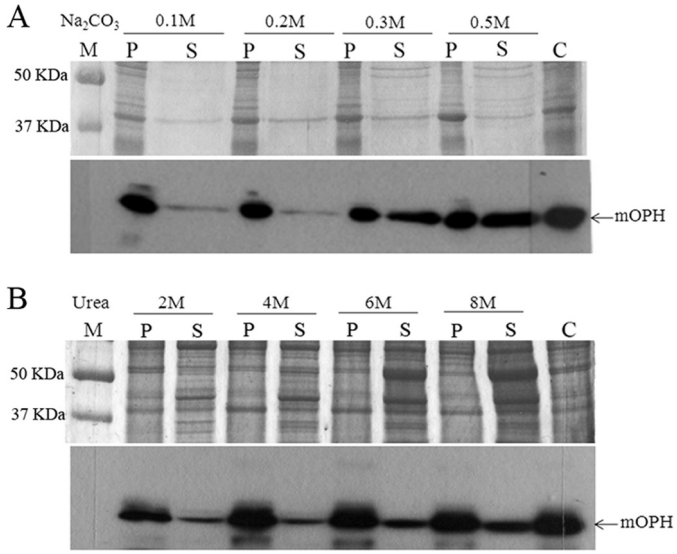

FIGURE 1. **OPH remains membrane-associated in the presence of sodium carbonate or urea.** Inner membranes isolated from *B. diminuta* cells were washed with increasing concentrations of either sodium carbonate (*panel A*) or urea (*panel B*), as indicated. The pellet (*P*) and supernatant (*S*) fractions after washing were separated by SDS-PAGE (12.5% acrylamide), and either stained with Coomassie Blue (*upper panels*) or blotted and probed with an OPH antibody (*lower panels*). The untreated membrane (*C*) is loaded along with the treated samples as a control. *M*, molecular weight marker.

Results

OPH Is Tightly Bound to the B. diminuta Inner Membrane—It has previously been demonstrated that OPH is associated with the inner membrane of *B. diminuta* (15). To probe the nature of the interaction of OPH with the membrane, we first determined whether the protein could be released from membrane fractions following washing under alkaline conditions using sodium carbonate (Fig. 1*A*), or under strong denaturing conditions in the presence of urea (Fig. 1*B*). At concentrations of sodium carbonate normally used to extract peripheral membrane proteins (0.1–0.5 M) (34), very little OPH was released from the membrane, suggesting a relatively tight association with the bilayer. However, at higher concentrations of carbonate, significant levels of OPH were released (Fig. 1*A*). Likewise the protein was also relatively refractory to extraction by urea, with most of the protein remaining associated with the membrane fraction even in the presence of 8 M urea (Fig. 1*B*). This behavior is consistent with OPH being an integral protein of the inner membrane rather than associating with the membrane by electrostatic interaction or through binding to other inner membrane proteins.

OPH Is a Lipoprotein—The Tat system is known to assemble some membrane-anchored proteins (20, 35, 36). In bacteria these usually have either a single transmembrane domain at the C terminus (35) or an N-terminal non-cleaved twin-arginine signal anchor sequence (37). However, bioinformatic analysis supported by structural studies show that OPH has no C-terminal hydrophobic helical domain (38) and the N-terminal signal peptide of OPH is cleaved off during biosynthesis and therefore cannot serve as a signal anchor (15).

A third class of bacterial membrane proteins that are known to be assembled by the Tat pathway is lipoproteins (20, 39, 40).

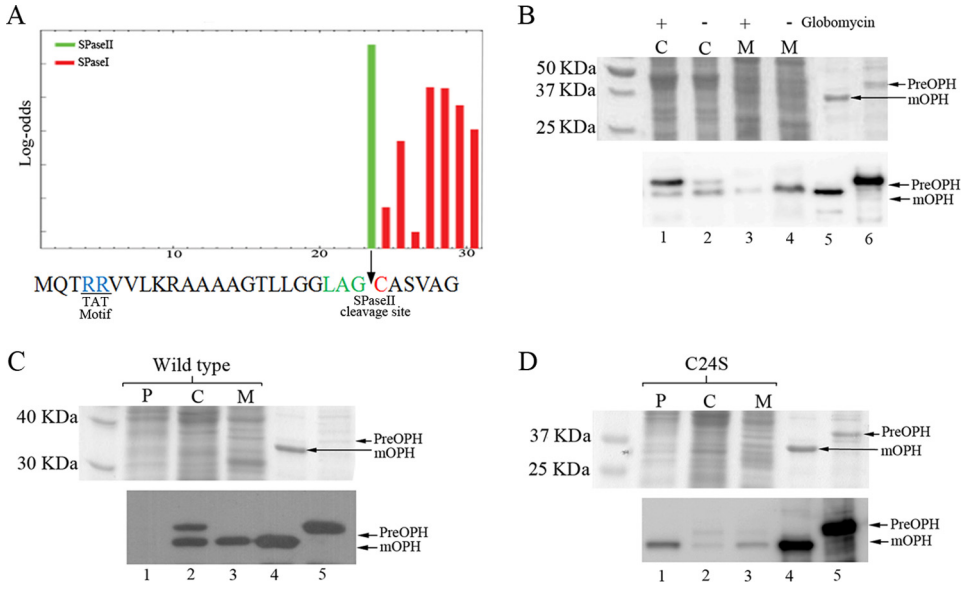

FIGURE 2. **OPH is a lipoprotein.** *A*, bioinformatic analysis of the OPH signal peptide. The predicted SPaseII cleavage site (*green bar*), lipo-box (*green font*), and the invariant cysteine residue (*red font*) found at the junction of the SPaseII cleavage site are shown. Potential SPaseI cleavage sites are indicated with *red bars*. The twin arginines of the Tat signal peptide are *underlined*. *B*, SDS-PAGE analysis (12.5% acrylamide; *upper panel*, shown as a loading control) and anti-OPH Western blot (*lower panel*) of membrane (*M*) and cytoplasmic (*C*) proteins extracted from globomycin-treated (+) and untreated (−) cells of *B. diminuta* DS010 (pSM5). *Lanes 5* and *6* show pure mOPH (*5*) and pre-OPH (*6*) used as molecular size markers. *C* and *D*, SDS-PAGE (12.5% acrylamide; *upper panel*) and corresponding Western blot (*lower panel*) of proteins extracted from periplasmic, cytoplasmic, and membrane fractions of *B. diminuta* DS010 containing (*C*) plasmid pSM5 that produces wild type OPH or (*D*) plasmid pCSOPH producing OPH^{C24S}. *Lanes 4* and *5* indicate mOPH (*4*) and pre-OPH (*5*) used as molecular size markers.

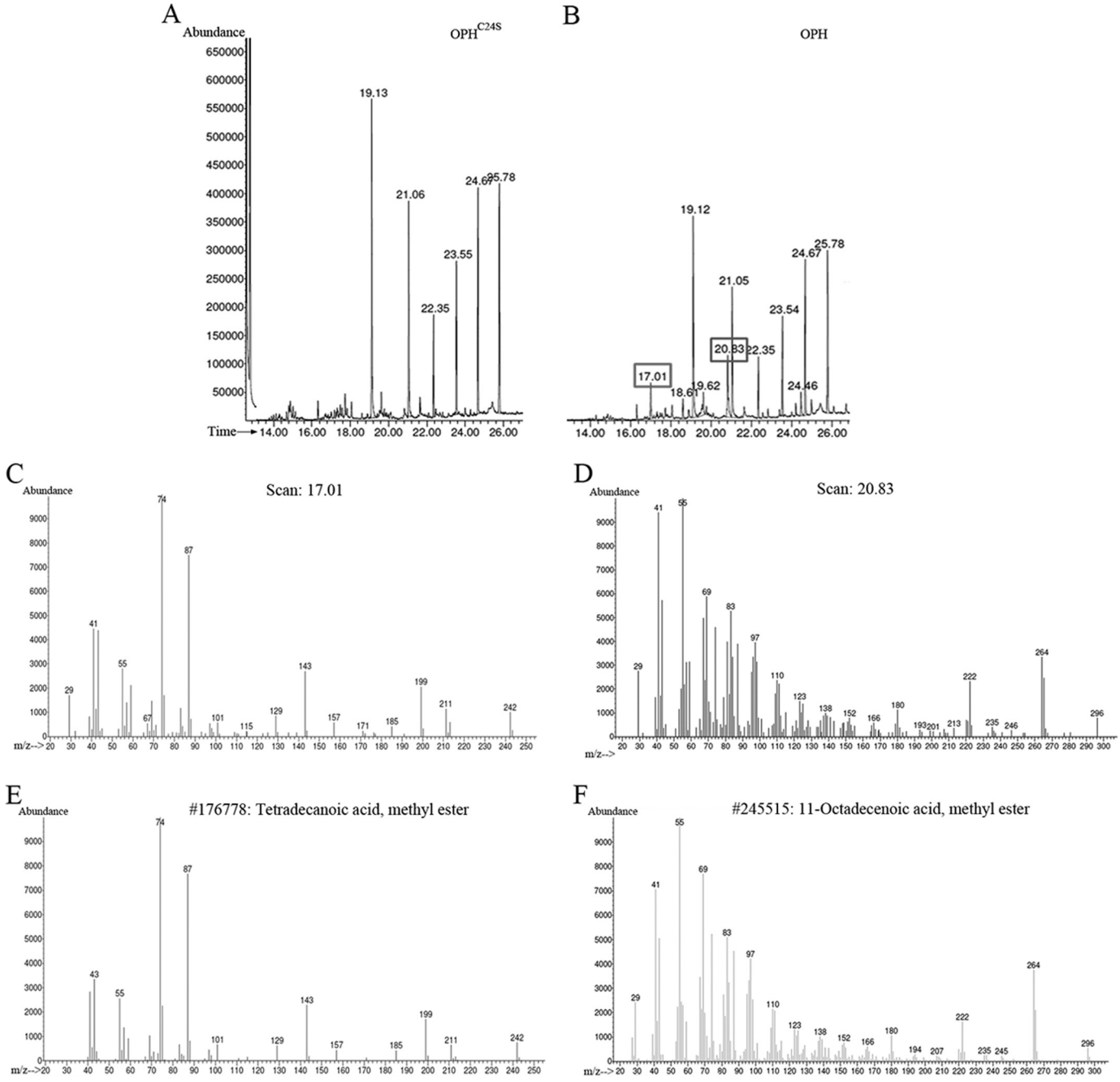

FIGURE 3. **Fatty acids associated with the invariant cysteine residue of OPH.** Gas chromatograms of the fatty acid methyl esters extracted from OPH^{C24S} (*A*) and wild type OPH (*B*). The novel fatty acid peaks found in the wild type OPH sample are highlighted with *boxes*. The MS pattern of novel peaks obtained at retention times of 17.01 (*C*) and 20.83 (*D*) and corresponding library search results are shown in *E* for the 17.01 peak and *F* for the 20.83 peak.

In silico analysis of the OPH signal peptide, shown in Fig. 2*A*, predicts the existence of both signal peptidase II (SpaseII) and multiple signal peptidase I (SpaseI) cleavage sites in pre-OPH, with the SpaseII cleavage site predicted with the highest level of confidence. In addition to the predicted SpaseII cleavage site, a well conserved lipobox containing a cysteine residue was found in the c-region of the signal peptide (Fig. 2*A*). To determine whether OPH was a substrate of SpaseII, we treated cells of *B. diminuta* DS010 (pSM5) with globomycin, which inhibits processing of the prolipoprotein by binding irreversibly to the peptidase (20, 41). In support of the *in silico* prediction, in the globomycin-treated cultures most of the OPH accumulated in the cytoplasmic fraction in an unprocessed form (Fig. 2*B*, *lane 1*). This is in contrast with the untreated cells where very little precursor was detectable (Fig. 2*B*, *lane 2*). Moreover, there was substantially less mature OPH detectable in the membrane fraction following globomycin treatment (Fig. 2*B*, *lane 3*).

To provide additional evidence that OPH is a lipoprotein, we generated a serine substitution of the essential cysteine in the OPH signal sequence lipobox (OPH^{C24S}) and compared the subcellular location of this variant to that of the wild type

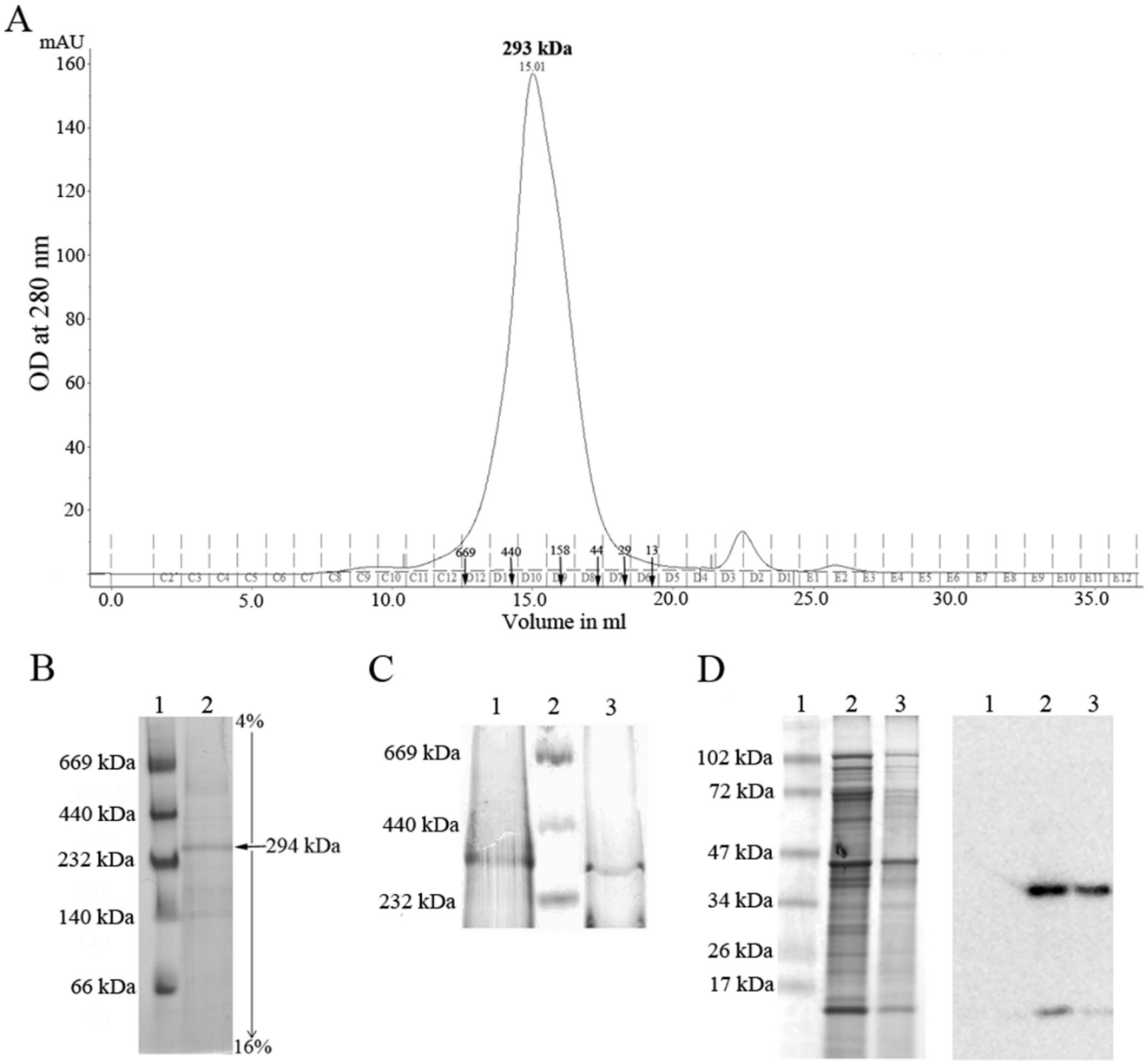

FIGURE 4. **Purification of an OPH complex.** *A* and *B,* molecular mass determination of the nickel affinity purified OPH complex from detergent-extracted membranes by (*A*) gel filtration and (*B*) BN-PAGE. *A,* the *bold inverted arrows* indicate elution volumes of thyroglobulin (669 kDa), ferritin (440 kDa), aldolase (158 kDa), ovalbumin (44 kDa), carbonic anhydrase (29 kDa), and ribonuclease (13 kDa) used to calibrate the column. *B*, BN-PAGE analysis (4–16% acrylamide) of IMAC purified OPH complex (*lane 2*). *Panels C* and *D* show BN-PAGE analysis of IMAC purified OPH complex (*C*) and Tricine-SDS-PAGE (*D*) analysis of the formaldehyde cross-linked OPH complex purified after delipidation by the extracting the membrane proteins with chloroform:methanol (1:3). *C,* the immunopurified OPH complex is shown in *lane 1* and the IMAC purified complex in *lane 3*. Molecular weight markers are in *lane 2*. *D,* Tricine-SDS-PAGE (4–16%) profile (*left*) and corresponding Western blots probed using anti-OPH antibodies (*right*) for immunopurified OPH complex (*lane 2*) and IMAC purified complex (*lane 3*). Molecular weight markers are in *lane 1*.

protein (Fig. 2, *C* and *D*). Unlike the wild type protein where the mature form is found in the membrane fraction (Fig. 2*C*), most of the processed form of OPH^{C24S} was found in periplasm, with very little seen in the membrane (Fig. 2*D*). Because SpaseII acts only on acylated prolipoproteins to generate S-lipidated cysteine at the N terminus of the mature protein (42), it is assumed that the mature-sized form of OPH^{C24S} found in the periplasmic fraction results from processing by SpaseI (Fig. 2*A*), which is predicted bioinformatically to recognize this signal peptide (Fig. 2*A*). Taken together these results demonstrate that OPH is a membrane-anchored lipoprotein.

Mature OPH Is Linked to Myristic and Oleic Fatty Acids—Previous findings have shown that generally diacyl glycerol serves as a lipid anchor for membrane-associated lipoproteins (43). To confirm the nature of the lipid anchor on membrane-bound OPH and to identify the fatty acid modifications, we extracted fatty acids from affinity purified OPH and OPH^{C24S} (as a negative control) using methanolic HCl extraction (24). The fatty acid methyl esters generated due to transesterification were extracted and analyzed using GC-MS. As shown in Fig. 3, *A* and *B*, two novel peaks were identified arising from the mOPH purified from *B. diminuta* membranes, which were not observed in the control sample derived from OPH^{C24S}. These

TABLE 3
Unique peptide sequences identified in OPH complex

Unique peptides	Peptide sequences	% Coverage	M_r	Accession	Description	Function	Subcellular localization
4	TIVDVSTFDIGR/ASLATGVPVTTHTAASQR/ VNPDGMAFIPLR/GVPQE TLAGITVTNPAR/	17	35.7	gi 13786716	Phosphotriesterase (*B. diminuta*)	Unusual substrate specificity for synthetic organophosphate triesters	Plasma membrane
4	SDLPDGILEPQVVR/VILDPAR/IATLGDIDQNAAK/ AVNDVNQAVQQIR	4.3	123.3	gi 103485965	AcrB, acriflavin resistance protein (*S. alaskensis* RB2256)	Transporter activity	Integral component of membrane
3	LEGVVASLASK/GLAGAFNSNIVK/ LTIQYNR	7.2	31	gi 103487768	F0F1 ATP synthase subunity (*S. alaskensis* RB2256)	Proton-transporting ATP synthase activity, rotational mechanism	Plasma membrane
2	FTQAGSEVSALLGR/ VIDLLAPYAR	2.5	53.9	gi 103487769	F0F1 ATP synthase subunitβ (*S. alaskensis* RB2256)	Proton-transporting ATP synthase activity, rotational mechanism	Plasma membrane
2	LELAQYR/LSVGDGIA	1.2	54.4	gi 103487767	F0F1 ATP synthase subunitα (*S. alaskensis* RB2256)	Proton-transporting ATP synthase activity, rotational mechanism	Plasma membrane
2	LALAEGDLR/VADPSFGVR	1.6	52.6	gi 103487743	Type I secretion outer membrane protein, TolC (*S. alaskensis* RB2256)	Outer membrane channel, required for several efflux systems such as AcrAB-TolC, AcrEF-TolC, EmrAB-TolC, and MacAB-TolC	Cell outer membrane
2	FDAAGVPNLK/VIGSPGYPAEEER	3	32.2	gi 103487703	α/β Hydrolase (*S. alaskensis* RB2256)	Hydrolase activity/ aromatic compounds	Unknown
2	LPAVAISVFG/ISAVGSSTV	3	34.2	gi 159795674	Phosphate preplasmic binding protein Psts (*Y. pestis*)	Phosphate binding periplamsic component	Periplasm

two peaks corresponded to methyl myristate (C14:0) and methyl oleic acid (C18:1) with 97 and 99% identities (Fig. 3, *C–F*). These results demonstrate that OPH is anchored to the membrane through diacylglycerol, which is linked with myristic and oleic groups.

OPH Interacts with Phosphate ABC Transporter—To gain further clues about the physiological role of OPH, we next sought to identify whether it interacted with other cellular proteins. First we developed a strategy to purify OPH in its native state by dispersing the membrane fraction with the non-ionic detergents Triton X-114, DDM, and digitonin. Of the three detergents, DDM facilitated the best release of OPH (liberating ~70% of total OPH; data not shown).

Next, we developed a strategy to purify DDM-solubilized OPH. In the crystal structure of OPH the C-terminal region is exposed (38), and we therefore constructed a strain of *B. diminuta* producing OPH with a C-terminal His_6 tag. However, the DDM-solubilized OPH^{C6His} failed to bind the nickel-nitrilotriacetic acid column, suggesting that the C terminus of OPH is not able to interact with the affinity matrix, possibly due to masking of this region by a partner protein subunit. To resolve this problem, we again used the crystal structure of OPH as a reference to introduce an internal His_{10} tag internally into a loop region of OPH. This variant, designated OPH^{10xHis}, bound well to the nickel-affinity matrix following solubilization from the membrane. The affinity-purified OPH^{10xHis} sample was further analyzed both by BN-PAGE and gel filtration. These two independent experiments both suggested that OPH^{10xHis} was present in a complex of around 294 kDa (Fig. 4, *A* and *B*). Assuming that the detergent used to solubilize OPH from the membrane may interfere with the determination of an accurate molecular mass for the OPH complex, the isolated membranes from the formaldehyde-treated *B. diminuta* DS010 (pOPH141HIS) cells were extracted with chloroform:methanol (1:3) to delipidate the sample and the resulting membrane protein precipitate was resolubilized before proceeding with affinity purification of the cross-linked OPH complex. BN-PAGE analysis of the OPH complex isolated in this way coincided with the mass of the OPH complex purified from detergent-solubilized membranes (compare Fig. 4, *B* with *C, lane 3*).

To validate these findings we employed a second, independent approach to purify untagged OPH. The membranes isolated from the formaldehyde cross-linked *B. diminuta* wild type cells were extracted with chloroform:methanol (1:3) and the resolubilized membrane proteins were passed through a protein A column that had been cross-linked with OPH-specific antibodies. The size of the OPH complex obtained following this purification process coincided with the BN-PAGE profile of the OPH complex purified following nickel-affinity column (IMAC) (Fig. 4*C*, *lane 3*). We therefore conclude that OPH is present in an ~293 kDa complex.

The delipidated OPH complexes purified by immunoaffinity and IMAC were analyzed by Tricine-SDS-PAGE. It can be seen (Fig. 4*D*) that several protein bands with similar sizes are common between the two samples, although bands with apparent masses of 38, 35, and 15 kDa are more intense in the immunopurified OPH complex. The 35-kDa protein coincided with the

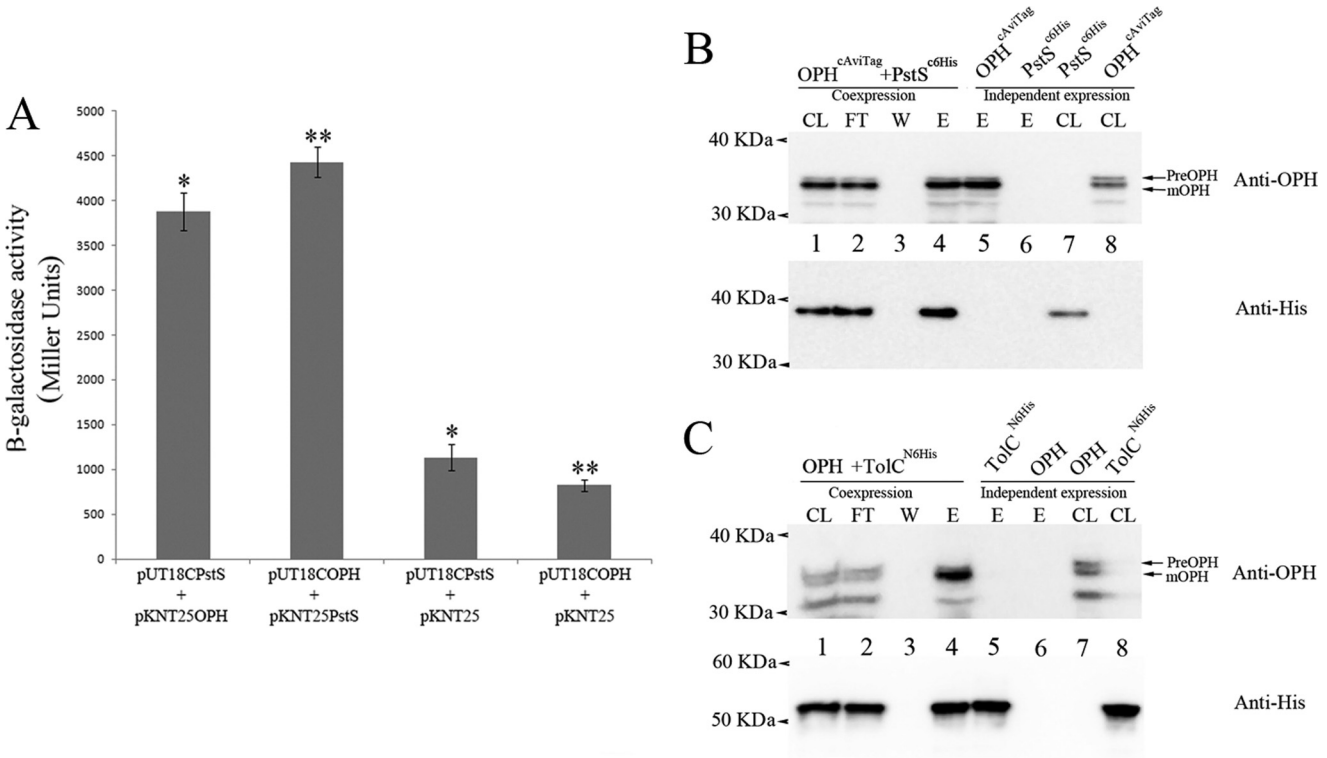

FIGURE 5. **OPH directly interacts with PstS and TolC.** *A,* interactions between the indicated variants of OPH and PstS fused to either the T18 or T25 fragments of *Bordetella pertussis* adenylate cyclase, as indicated. *Error bars* represent the mean ± S.E. ($n = 3$). Also shown are controls performed with either OPH or PstS fused to the T18 fragment tested against the unfused T25 fragment. Significance was assessed using Student's *t* test, where * signifies $p < 0.0001$ and ** signifies $p < 0.0001$ relative to the value for T18-PstS + T25 and T18-OPH + T25, respectively. *B,* tagged variants of OPH and PstS copurify. The Western blotting for SDS-PAGE (12.5% acrylamide), probed with anti-OPH (*top panel*) or anti-His antibodies (*bottom panel*) show cell lysate (*CL*) of *E. coli* strain ArcticExpress producing $OPH^{CaviTag}$, BirA, and $PstS^{C6His}$ (*lane 1*), incubated with streptavidin magnetic beads. *FT*, flow-through (*lane 2*); *W*, wash fraction (*lane 3*); and *E*, eluted bound protein from the beads (*lane 4*). *Lanes 5–8* represent control lanes showing elution (*E*) of bound protein when the streptavidin magnetic beads were incubated with the ArcticExpress cell lysates prepared from the cultures induced to express $OPH^{CaviTag}$, BirA only (*lane 5*), or $PstS^{C6His}$ (*lane 6*). The total cell lysates expressing $PstS^{C6His}$ (*lane 7*) and $OPH^{CaviTag}$ (*lane 8*) were loaded as positive controls. *C,* OPH copurifies with His-tagged TolC. Lysates of ArcticExpress producing OPH and $TolC^{N6His}$ (*lane 1*) were incubated with nickel-nitrilotriacetic acid magnetic beads. *FT*, flow-through (*lane 2*); *W*, wash fraction (*lane 3*); and *E*, eluted bound protein from the beads (*lane 4*) were analyzed by SDS-PAGE (12.5% acrylamide). *Lanes 5* and *6* are controls showing eluted proteins bound to the nickel-nitrilotriacetic acid magnetic beads incubated with the lysates prepared from the ArcticExpress cells expressing OPH and $TolC^{N6His}$. Total cell lysates having OPH (*lane 7*) and $TolC^{N6His}$ (*lane 8*) are loaded as positive controls.

size of OPH and its identity was also established by performing a Western immunoblot with anti-OPH antibodies (Fig. 4*D*).

After establishing that OPH is a multiprotein complex, we performed mass spectrometry to obtain unique peptide sequences from proteins copurifying with OPH following IMAC. The obtained peptide sequences were identified using either x!tandem or Mascot web servers. Proteins that matched with more than two peptide sequences are listed in Table 3. From the list of proteins, subunits of the F_1F_o-ATP synthase (α, β, γ), the phosphate ABC transporter substrate-binding protein (PstS) and efflux pump components AcrB and TolC were identified as candidate OPH interacting partners (Table 3). It is interesting to note that the identified peptides matched with proteins involved either in phosphate uptake (44) or in effluxing of xenobiotics (45), as organophosphates are xenobiotics that also contain a potential source of phosphate.

OPH Interacts with Phosphate-specific Transport Component PstS—As PstS is a periplasmic protein that binds specifically to inorganic phosphate, we chose to further probe potential interaction of OPH with PstS. Initially we undertook bacterial two-hybrid analysis to assess OPH-PstS interactions. When PstS was fused to the C terminus of the adenylate cyclase T18 fragment and OPH to the N terminus of the T25 fragment, adenylate cyclase activity was reconstituted, and strong β-galactosidase activity could be measured (Fig. 5*A*). A similar strong interaction was also seen when OPH was fused to the C terminus of the adenylate cyclase T18 fragment and PstS to the N terminus of the T25 fragment. To confirm that OPH and PstS directly interact, we performed coexpression pulldown assays. To this end we generated compatible plasmids coding for $OPH^{CAviTag}$ (pAVB400) and $PstS^{N6His}$ (pPST300). In addition, plasmid pAVB400 also codes for the biotin ligase, BirA, to facilitate ligation of biotin at the conserved lysine residue of AviTag found at the C terminus of $OPH^{CAviTag}$. After inducing the production of $OPH^{CAviTag}$, $PstS^{N6His}$, and biotin ligase in the heterologous host *E. coli*, streptavidin-linked beads were used to isolate biotinylated $OPH^{CAviTag}$. As shown in Fig. 5*B*, $PstS^{N6His}$ copurified with the biotinylated $OPH^{CAviTag}$ (Fig. 5*B, lane 4*), but was not purified by the streptavidin-linked beads in the absence of $OPH^{CAviTag}$ (Fig. 5*B*, *lane 6*), providing conclusive proof that OPH and PstS are interaction partners.

Efflux Pump Component TolC Interacts with OPH—Analysis of the OPH interactome indicated that efflux pump components AcrA, AcrB, and TolC also copurified with OPH isolated from *B. diminuta* (Table 3). We next sought to assess whether there was a direct interaction between OPH and any of these

three proteins by heterologous expression and pairwise copurification studies. Unfortunately, we were unable to express *B. diminuta* AcrA and AcrB in *E. coli*. However, TolC with an N-terminal His tag was successfully produced in the *E. coli* ArcticExpress strain. We therefore coexpressed untagged OPH along with $TolC^{N6His}$ and isolated $TolC^{N6His}$ from total cell lysates using MagneHis beads. Fig. 5*C* shows that when $TolC^{N6His}$ was affinity purified, the mature form of OPH was also copurified (Fig. 5*C*, *lane 4*). Because OPH produced in the absence of $TolC^{N6His}$ was unable to interact with the beads (Fig. 5*C*, *lane 6*), it can be concluded that OPH and TolC can directly interact with each other.

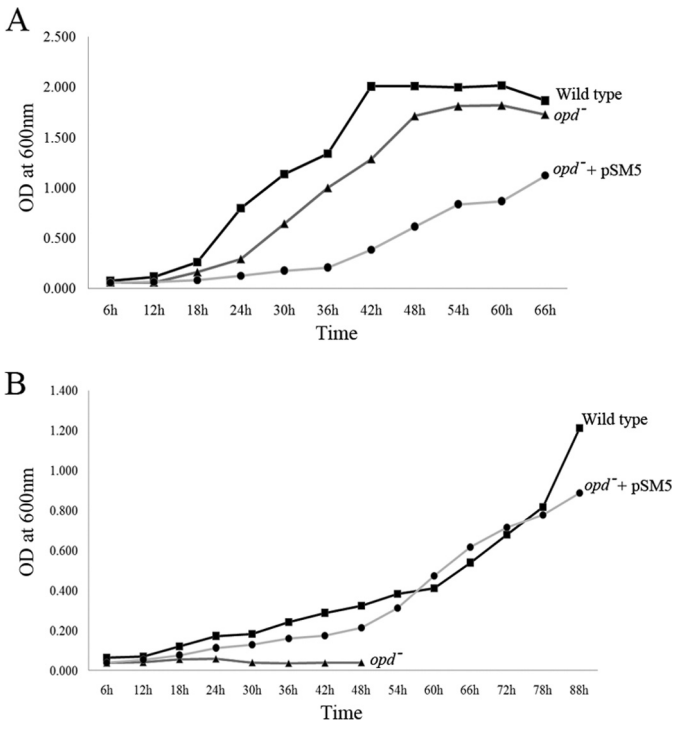

FIGURE 6. **OPH supports growth of *B. diminuta* using the organophosphate methyl parathion as sole phosphate source.** *Panels A* and *B* show growth of *B. diminuta* wild type (■), DS010 (▲), and DS010 (pSM5) (●) in minimal medium having either $(NH_4)_2HPO_4$ (*panel A*) or methyl parathion as sole phosphate source (*panel B*).

OPH Supports B. diminuta Growth with Methyl Parathion as Sole Phosphate Source—The enzymatic action of OPH generates alkyl phosphates from a variety of organophosphate insecticides due to its triesterase activity (3). These diesters, like diethyl phosphate, may serve as substrates for periplasmically located phosphatases/diesterases, ultimately generating inorganic phosphate (P_i), raising the possibility that interaction of OPH with PstS facilitates the transport of generated inorganic phosphate into the cell. To examine this further, we investigated the ability of *B. diminuta* to grow in minimal medium using the OP insecticide methyl parathion as sole source of phosphate. As shown in Fig. 6, *B. diminuta* DS010 alone was unable to grow using methyl parathion as phosphate source, but when carrying plasmid pSM5, encoding OPH, good growth was seen. These results show that OPH is required to support growth using organophosphates as a source of phosphate.

Discussion

In this study we have investigated the interaction of the organophosphate hydrolase, OPH, from *B. diminuta*, with the cytoplasmic membrane and with other cellular proteins. Our work has clearly shown that OPH is a lipoprotein, and adds to a growing list of Tat-dependent lipoproteins in bacteria and archaea (20, 44, 47, 48). Interestingly, OPH contains an alanine residue at the +2 position and according to the sorting rules for *E. coli* lipoproteins (42) should be translocated to the outer

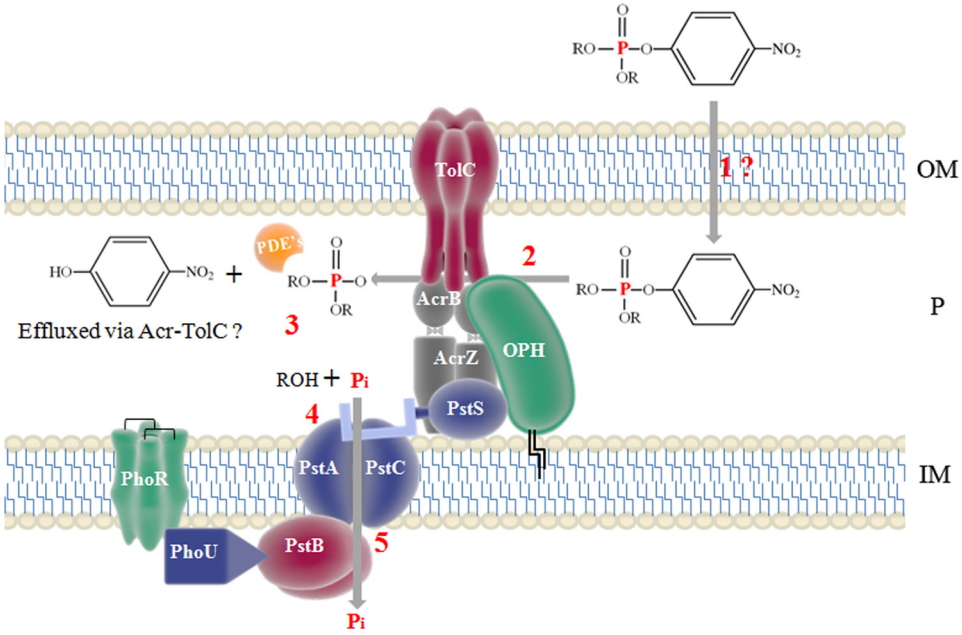

FIGURE 7. **Model for OPH-mediated phosphate acquisition in *B. diminuta*.** The model includes OPH and its interacting partners TolC, AcrA, PstS, and PhoR. The other components of the ABC-type phosphate acquisition system (PstA, PstB, and PstC) for which PstS is the periplasmic binding protein are also shown. Entry of the model OP compound to periplasm (*1*) and its OPH-mediated hydrolysis (*2*) generate alkyl phosphate and *p*-nitrophenol. P_i is generated through the action of periplasmically located phosphatases/diesterases (*3*), which binds to PstS (*4*) and is transported into the cytoplasm by the phosphate-specific transport system (*5*). *OM*, outer membrane; *P*, periplasm; *IM*, inner membrane.

membrane by the Lol machinery (the genes for which are found in the genome of *B. diminuta*). However, a number of exceptions to these sorting "rules" have been seen in other Gram-negative bacteria, for example, in *Pseudomonas aeruginosa* where lipoproteins having lysine, glycine, and glutamine at the +2 position remain attached to the inner membrane (49). It appears for *B. diminuta* an alanine at the +2 position also permits inner membrane retention.

Copurification studies using two independent approaches showed that OPH was present as a large multiprotein complex that includes other inner membrane proteins such as a predicted PhoR-like histidine kinase, periplasmic proteins such as PstS, and outer membrane proteins TolC and AcrA. Further support for an OPH complex was provided by demonstrating a direct interaction between OPH and PstS, and between OPH and TolC. Growth studies showed that the indirect liberation of organic phosphates from methyl parathion mediated by OPH can support growth with this compound as the sole phosphate source. These findings point to a potential model whereby the triesterase activity of OPH generates phosphodiesters from a variety of OP insecticides, which are converted to inorganic phosphates by periplasmically located phosphatases (Fig. 7). The PstS protein, identified here as an interacting partner of OPH, is a known component of an established phosphotransfer system (44), and it binds to inorganic phosphate, facilitating its transport across the inner membrane. During OPH-mediated hydrolysis of OP insecticides, in addition to alkyl phosphates, aromatic compounds like *p*-nitrophenol are also generated. Products such as *p*-nitrophenol are more toxic than the parent compounds and if they are not quickly metabolized they need to be effluxed for the survival of the organism. In this context, OPH interactions with efflux pumps may serve to quickly eliminate toxic degradation products from the intracellular environment.

Author Contributions—S. P., H. P., and A. N. performed the experiments. T. P. and D. S. conceived the idea and drafted the manuscript.

Acknowledgment—We thank Prof. P. S. Sastry for critical inputs.

References

1. Cho, C. M., Mulchandani, A., and Chen, W. (2002) Bacterial cell surface display of organophosphorus hydrolase for selective screening of improved hydrolysis of organophosphate nerve agents. *Appl. Environ. Microbiol.* **68,** 2026–2030
2. Efrmenko, E. N., and Sergeeva, V. S. (2001) Organophosphate hydrolase: an enzyme catalyzing degradation of phosphorus-containing toxins and pesticides. *Russ. Chem. Bull. (Int. Ed)*. **50,** 1826–1832
3. Dumas, D. P., Caldwell, S. R., Wild, J. R., and Raushel, F. M. (1989) Purification and Properties of the Phosphotriesterase from *Pseudomonas diminuta*. *J. Biol. Chem.* **264,** 19659–19665
4. Pandeeti, E. V. P., Longkumer, T., Chakka, D., Muthyala, V. R., Parthasarathy, S., Madugundu, A. K., Ghanta, S., Medipally, S. R., Pantula, S. C., Yekkala, H., and Siddavattam, D. (2012) Multiple mechanisms contribute to lateral transfer of an organophosphate degradation (*opd*) island in *Sphingobium fuliginis* ATCC 27551. *G3 (Bethesda)* **2,** 1541–1554
5. Pandeeti, E. V., Chakka, D., Pandey, J. P., and Siddavattam, D. (2011) Indigenous organophosphate-degrading (opd) plasmid pCMS1 of *Brevundimonas diminuta* is self-transmissible and plays a key role in horizontal mobility of the *opd* gene. *Plasmid* **65,** 226–231
6. Omburo, G. A., Kuo, J. M., Mullins, L. S., and Raushel, F. M. (1992) Characterization of the zinc binding site of bacterial phosphotriesterase. *J. Biol. Chem.* **267,** 13278–13283
7. Walker, C. H. (1993) The classification of esterases which hydrolyse organophosphates: Recent developments. *Chem. Biol. Interact.* **87,** 17–24
8. Bigley, A. N., and Raushel, F. M. (2013) Catalytic mechanisms for phosphotriesterases. *Biochim. Biophys. Acta* **1834,** 443–453
9. Brown, K. A. (1980) Phosphotriesterases of *Flavobacterium* sp. *Soil Biol. Biochem.* **12,** 105–112
10. Chaudhry, G. R., Ali, A. N., and Wheeler, W. B. (1988) Isolation of a methyl parathion-degrading *Pseudomonas* sp. that possesses DNA homologous to the *opd* gene from a *Flavobacterium* sp. *Appl. Environ. Microbiol.* **54,** 288–293
11. Serdar, C. M., Gibson, D. T., Munnecke, D. M., and Lancaster, J. H. (1982) Plasmid involvement in parathion hydrolysis by *Pseudomonas diminuta*. *Appl. Environ. Microbiol.* **44,** 246–249
12. Mulbry, W. W., and Karns, J. S. (1989) Purification and characterization of three parathion hydrolases from Gram-negative bacterial strains. *Appl. Environ. Microbiol.* **55,** 289–293
13. Siddavattam, D., Khajamohiddin, S., Manavathi, B., Pakala, S. B., and Merrick, M. (2003) Transposon-like organization of the plasmid-borne organophosphate degradation (*opd*) gene cluster found in *Flavobacterium* sp. *Appl. Environ. Microbiol.* **69,** 2533–2539
14. Palmer, T., and Berks, B. C. (2012) The twin-arginine translocation (Tat) protein export pathway. *Nat. Rev. Microbiol.* **10,** 483–496
15. Gorla, P., Pandey, J. P., Parthasarathy, S., Merrick, M., and Siddavattam, D. (2009) Organophosphate hydrolase in *Brevundimonas diminuta* is targeted to the periplasmic face of the inner membrane by the twin arginine translocation pathway. *J. Bacteriol.* **191,** 6292–6299
16. Sambrook, and Russell, D. W. (eds) (2001) *Molecular Cloning: A Laboratory Manual* 1st Ed, Cold Spring Harbor Laboratory Press, Cold Spring Harbor, NY
17. Kaback, H. R. (1971) Bacterial membranes. *Methods Enzymol.* **22,** 99–120
18. Schnaitmann, C. A. (1970) Protein composition of the cell wall and cytoplasmic membrane of *Escherichia coli*. *J. Bacteriol.* **104,** 890–901
19. Zwiebel, L. J., Inukai, M., Nakamura, K., and Inouye, M. (1981) Preferential selection of deletion mutations of the outer membrane lipoprotein gene of *Escherichia coli* by globomycin. *J. Bacteriol.* **145,** 654–656
20. Giménez, M. I., Dilks, K., and Pohlschröder, M. (2007) Haloferax volcanii twin-arginine translocation substates include secreted soluble, C-terminally anchored and lipoproteins. *Mol. Microbiol.* **66,** 1597–1606
21. van Geest, M., and Lolkema, J. S. (1996) Membrane topology of the sodium ion-dependent citrate carrier of *Klebsiella pneumonia*: evidence for a new structural class of secondary transporters. *J. Biol. Chem.* **271,** 25582–25589
22. Weiner, J. H., Bilous, P. T., Shaw, G. M., Lubitz, S. P., Frost, L., Thomas, G. H., Cole, J. A., and Turner, R. J. (1998) A novel and ubiquitous system for membrane targeting and secretion of cofactor-containing proteins. *Cell* **93,** 93–101
23. Kanugula, A. K., Repalle, E. R., Pandey, J. P., Sripad, G., Mitra, C. K., Dubey, D. K., and Siddavattam, D. (2011) Immobilization of organophosphate hydrolase on biocompatible gelatine pads and its use in removal of organophosphate compounds and nerve agents. *Indian J. Biochem. Biophys.* **48,** 29–34
24. Ichihara, K., and Fukubayashi, Y. (2010) Preparation of fatty acid methyl esters for gas-liquid chromatography. *J. Lipid Res.* **51,** 635–640
25. Nadeau O. W., and Carlson G. M. (2007) Protein interactions captured by chemical cross-linking: one-step cross-linking with formaldehyde. *CSH Protoc.* **2007,** pdb.prot4634
26. Sutherland, B. W., Toews, J., and Kast, J. (2008) Utility of formaldehyde cross-linking and mass spectrometry in the study of protein-protein interactions. *J. Mass. Spectrom.* **43,** 699–715
27. Poole, R. K. (1993) The isolation of membranes from bacteria: biomembrane protocols. *Methods Mol. Biol.* **19,** 109–122
28. Schägger, H., and von Jagow, G. (1991) Blue native electrophoresis for isolation of membrane protein complexes in enzymatically active form. *Anal. Biochem.* **199,** 223–231
29. Schägger, H. (2006) Tricine–SDS-PAGE. *Nat. Protoc.* **1,** 16–22

30. Kim, M. S., Kandasamy, K., Chaerkady, R., and Pandey, A. (2010) Assessment of resolution parameters for CID-based shotgun proteomic experiments on the LTQ-Orbitrap mass spectrometer. *J. Am. Soc. Mass. Spectrom.* **21,** 1606–1611
31. Karimova, G., Pidoux, J., Ullmann, A., and Ladant, D. (1998) A bacterial two-hybrid system based on a reconstituted signal transduction pathway. *Proc. Natl. Acad. Sci.* **95,** 5752–5756
32. Zhang, X., and Bremer, H. (1995) Control of the *Escherichia coli* rrnB P1 promoter strength by ppGpp. *J. Biol. Chem.* **270,** 11181–11189
33. Müllerová, D., Krajčíková, D., and Barák, I. (2009) Interactions between *Bacillus subtilis* early spore coat morphogenetic proteins. *FEMS Microbiol. Lett.* **299,** 74–85
34. Molloy, M. P., Herbert, B. R., Slade, M. B., Rabilloud, T., Nouwens, A. S., Williams, K. L., and Gooley, A. A. (2000) Proteomic analysis of the *Escherichia coli* outer membrane. *Eur. J. Biochem.* **267,** 2871–2881
35. Hatzixanthis, K., Palmer, T., and Sargent, F. (2003) A subset of bacterial inner membrane proteins integrated by the twin-arginine translocase. *Mol. Microbiol.* **49,** 1377–1390
36. Keller, R., de Keyzer, J., Driessen, A. J., and Palmer, T. (2012) Co-operation between different targeting pathways during integration of a membrane protein. *J. Cell Biol.* **199,** 303–315
37. Bachmann, J., Bauer, B., Zwicker, K., Ludwig, B., and Anderka, O. (2006) The Rieske protein from *Paracoccus denitrificans* is inserted into the cytoplasmic membrane by the twin-arginine translocase. *FEBS J.* **273,** 4817–4830
38. Benning, M. M., Shim, H., Raushel, F. M., and Holden, H. M. (2001) High resolution x-ray structures of different metal-substituted forms of phosphotriesterase from *Pseudomonas diminuta*. *Biochemistry* **40,** 2712–2722
39. Thompson, B. J., Widdick, D. A., Hicks, M. G., Chandra, G., Sutcliffe, I. C., Palmer, T., and Hutchings, M. I. (2010) Investigating lipoprotein biogenesis and function in the model Gram-positive bacterium *Streptomyces coelicolor*. *Mol. Microbiol.* **77,** 943–957
40. Widdick, D. A., Hicks, M. G., Thompson, B. J., Tschumi, A., Chandra, G., Sutcliffe, I. C., Brülle, J. K., Sander, P., Palmer, T., and Hutchings, M. I. (2011) Dissecting the complete lipoprotein biogenesis pathway in *Streptomyces scabies*. *Mol. Microbiol.* **80,** 1395–1412
41. Béven, L., Le Hénaff, M., Fontenelle, C., and Wróblewski, H. (1996) Inhibition of spiralin processing by the lipopeptide antibiotic globomycin. *Curr. Microbiol.* **33,** 317–322
42. Narita, S., and Tokuda, H. (2006) An ABC transporter mediating the membrane detachment of bacterial lipoproteins depending on their sorting signals. *FEBS Lett.* **580,** 1164–1170
43. Sankaran, K., and Wu, H. C. (1994) Lipid modification of bacterial prolipoprotein: transfer of diacylglyceryl moiety from phosphatidylglycerol. *J. Biol. Chem.* **269,** 19701–19706
44. Rao, N. N., and Torriani, A. (1990) Molecular aspects of phosphate transport in *Escherichia coli*. *Mol. Microbiol.* **4,** 1083–1090
45. Hobbs, E. C., Yin, X., Paul, B. J., Astarita, J. L., and Storz, G. (2012) Conserved small protein associates with the multidrug efflux pump AcrB and differentially affects antibiotic resistance. *Proc. Natl. Acad Sci. U.S.A.* **109,** 16696–16701
46. Siddavattam, D., Raju, E. R., Paul, P. V., and Merrick, M. (2006) Overexpression of parathion hydrolase in *Escherichia coli* stimulates the synthesis of outer membrane porin OmpF. *Pestic. Biochem. Physiol.* **86,** 146–150
47. Widdick, D. A., Dilks, K., Chandra, G., Bottrill, A., Naldrett, M., Pohlschröder, M., and Palmer, T. (2006) The twin-arginine translocation pathway is a major route of protein export in *Streptomyces coelicolor*. *Proc. Natl. Acad. Sci. U.S.A.* **103,** 17927–17932
48. Valente, F. M., Pereira, P. M., Venceslau, S. S., Regalla, M., Coelho, A. V., and Pereira, I. A. (2007) The [NiFeSe] hydrogenase from *Desulfovibrio vulgaris* Hildenborough is a bacterial lipoprotein lacking a typical lipoprotein signal peptide. *FEBS Lett.* **581,** 3341–3344
49. Tanaka, S. Y., Narita, S., and Tokuda, H. (2007) Characterization of the *Pseudomonas aeruginosa* Lol system as a lipoprotein sorting mechanism. *J. Biol. Chem.* **282,** 13379–13384
50. Hanahan, D. (1983) Studies on transformation of *Escherichia coli* with plasmids. *J. Mol. Biol.* **166,** 557–580
51. Studier, F. W., and Moffatt, B. A. (1986) Use of bacteriophage T7 RNA polymerase to direct selective high-level expression of cloned genes. *J. Mol. Biol.* **189,** 113–130
52. Simon, R., Priefer, U., and Pühler, A. (1983)A broad host range mobilization system for *in vivo* genetic engineering: transposon mutagenesis in Gram negative bacteria. *Nat. Biotechnol.* **1,** 784–791
53. Karimova, G., Dautin, N., and Ladant, D. (2005) Interaction network among *Escherichia coli* membrane proteins involved in cell division as revealed by bacterial two-hybrid analysis. *J. Bacteriol.* **187,** 2233–2243
54. Morales, V. M., Bäckman, A., and Bagdasarian, M. (1991) A series of wide-host-range low-copy number vectors that allow direct screening for recombinants. *Gene* **97,** 39–47

Organophosphate Hydrolase Is a Lipoprotein and Interacts with P_i-specific Transport System to Facilitate Growth of *Brevundimonas diminuta* Using OP Insecticide as Source of Phosphate

Sunil Parthasarathy, Hari Parapatla, Aparna Nandavaram, Tracy Palmer and Dayananda Siddavattam

J. Biol. Chem. 2016, 291:7774-7785.
doi: 10.1074/jbc.M116.715110 originally published online February 9, 2016
